2013

Assess the Accuracy of the Variational Asymptotic Plate and Shell Analysis Using the Generalized Uni

Luciano Demasi

Wenbin Yu
Utah State University

Recommended Citation
Luciano Demasi & Wenbin Yu (2013): Assess the Accuracy of the Variational Asymptotic Plate and Shell Analysis Using the Generalized Unified Formulation, Mechanics of Advanced Materials and Structures, 20:3, 227-241

Assess the Accuracy of the Variational Asymptotic Plate and Shell Analysis Using the Generalized Unified Formulation

Luciano Demasi [1]

Department of Aerospace Engineering & Engineering Mechanics
San Diego State University, San diego, CA 92182-1308 USA

Wenbin Yu

Department of Mechanical and Aerospace Engineering
Utah state University, Logan, Utah 84322-4130 USA

Abstract

The accuracy of the Variational Asymptotic Plate and Shell Analysis (VAPAS) is assessed against several higher order, zig zag and layerwise theories generated by using the invariant axiomatic framework denoted as Generalized Unified Formulation (GUF). These theories are also compared against the elasticity solution developed for the case of a sandwich structure with high Face to Core Stiffness Ratio. GUF allows to use an infinite number of axiomatic theories (Equivalent Single Layer theories with or without zig zag effects and Layerwise theories as well) with any combination of orders of the displacements and it is an ideal tool to precisely assess the range of applicability of the Variational Asymptotic Plate and Shell Analysis or other theories in general. In fact, all the axiomatic theories generated by GUF are obtained from the kernels or fundamental nuclei of the Generalized Unified Formulation and changing the order of the variables is "naturally" and systematically done with GUF. It is demonstrated that VAPAS achieves accuracy comparable to a fourth (or higher) order zig-zag theory or lower-order layerwise theories with the least number degrees of freedom. The differences between the axiomatic Zig-zag models and VAPAS are also assessed. Range of applicability of VAPAS will be discussed in detail and guidelines for new developments based on GUF and VAPAS are provided.

Email addresses: ldemasi@mail.sdsu.edu (Luciano Demasi), wenbin.yu@usu.edu (Wenbin Yu).

URLs: www.lucianodemasi.com (Luciano Demasi), http://www.mae.usu.edu/faculty/wenbin (Wenbin Yu).

[1] Corresponding author. Department of Aerospace Engineering and Engineering Mechanics, College of Engineering San Diego State University, 5500 Campanile Drive, San diego, CA 92182-1308

1 Introduction

1.1 Background and Motivation

Most of the aerospace structures can be analyzed using shell and plate models. Accurate theoretical formulations that minimize the CPU time without penalties on the quality of the results are then of fundamental importance.

The so-called axiomatic models present the advantage that the important physical behaviors of the structures can be modeled using the "intuition" of eminent scientists. The drawback of this approach is that some cases are not adequately modeled because the starting apriori assumptions might fail. Also, each existing approach presents a range of applicability and when the hypotheses used to formulate the theory are no longer valid the approach has to be replaced with another one usually named as "refined theory" or "improved theory". In the framework of the mechanical case, the Classical Plate Theory (CPT), also known as Kirchoff theory [22], has the advantage of being simple and reliable for thin plates. However, if there is strong anisotropy of the mechanic properties, or if the composite plate is relatively thick, other advanced models such as First-order Shear Deformation Theory (FSDT) are required [31, 26, 25]. Higher-order Shear Deformation Theories (HSDT) have also been used [35, 21, 41], giving the possibility to increase the accuracy of numerical evaluations for moderately thick plates. But even these theories are not sufficient if local effects are important or accuracy in the calculation of transverse stresses is sought. Therefore, more advanced plate theories have been developed to include zig-zag effects [27, 23, 4, 3, 1, 2, 32, 33, 14, 10, 24, 18]. In some challenging cases the previous type of theories are not sufficiently accurate. Therefore, the so-called Layerwise theories [13, 28, 34, 30, 9, 7, 8, 36, 19, 29, 11] have been introduced. In these theories the quantities are layer-dependent and the number of required Degrees of Freedom is much higher than the case of Equivalent Single Layer Models.

The first author introduced an invariant methodology named as Generalized Unified Formulation [16] in which an infinite number of axiomatic models can be included in just one formulation. All the combinations of orders (for example cubic order for the in-plane displacements and parabolic order for the out-of-plane displacement) are possible. Equivalent Single Layer Models (with or without zig-zag effects) and layerwise models can be analyzed. All these formulations derive from the expansion of six 1×1 arrays which are invariant with respect to the type of theory (e.g. Equivalent Single Layer or Layerwise) and orders adopted for the displacement variables. This fact makes the Generalized Unified Formulation an ideal tool to test and compare other possible formulations. In particular, this paper assesses the Variational Asymptotic Plate and Shell Analysis (VAPAS) introduced by the second author and his-coworkers

and compares it with some of the infinite theories that can be generated from the six invariant arrays of the Generalized Unified Formulation. All the results are compared against the elasticity solution developed by the first author. A sandwich plate is analyzed. Different aspect ratios are considered. Different Face to Core Stiffness ratios (FCSRs) are adopted. It is demonstrated that VAPAS gives accurate results at least as a fourth-order axiomatic zig-zag theory but with a much smaller number of Degrees of Freedom, except for some sandwich plates with huge FCSRs. The range of applicability of the various theories generated with GUF and VAPAS is discussed.

2 Variational Asymptotic Plate and Shell Analysis

Mathematically, the approximation in the process of constructing a plate theory stems from elimination of the thickness coordinate as an independent variable of the governing equations, a dimensional reduction process. This sort of approximation is inevitable if one wants to take advantage of the relative smallness of the thickness to simplify the analysis. However, other approximations that are not absolutely necessary should be avoided, if at all possible. For example, for geometrically nonlinear analysis of plates, it is reasonable to assume that the thickness, h, is small compared to the wavelength of deformation of the reference plane, l. However, it is unnecessary to assume *a priori* some displacement field, although that is the way most plate theories are constructed. As pointed out by Ref. [5], the attraction of *a priori* hypotheses is caused by our inability to extract the necessary information from the 3D energy expression.

According to this line of logic, Yu and his co-workers adopted the variational asymptotic method (VAM) [5], to develop a new approach to modeling composite laminates [39, 40, 38, 37]. These models are implemented in a computer program named VAPAS. In this approach, the original 3D anisotropic elasticity problem is first cast in an intrinsic form, so that the theory can accommodate arbitrarily large displacement and global rotation subject only to the strain being small. An energy functional can be constructed for this nonlinear 3D problem in terms of 2D generalized strain measures and warping functions describing the deformation of the transverse normal:

$$\Pi = \Pi(\epsilon_{11}, \epsilon_{12}, \epsilon_{22}, \kappa_{11}, \kappa_{12}, \kappa_{22}, w_1, w_2, w_3) \tag{1}$$

Here $\epsilon_{11}, \epsilon_{12}, \epsilon_{22}, \kappa_{11}, \kappa_{12}, \kappa_{22}$ are the so-called 2D generalized strains [20] and w_1, w_2, w_3 are unknown 3D warping functions, which characterize the difference between the deformation represented by the 2D variables and the actual 3D deformation for every material point within the plate. It is emphasized

here that the warping functions are not assumed *a priori* but are unknown 3D functions to be solved using VAM. Then we can employ VAM to asymptotically expand the 3D energy functional into a series of 2D functionals in terms of the small parameter h/l, such that

$$\Pi = \Pi_0 + \Pi_1 \frac{h}{l} + \Pi_2 \frac{h^2}{l^2} + o(\frac{h^2}{l^2}) \tag{2}$$

where Π_0, Π_1, Π_2 are governing functionals for different orders of approximation and are functions of 2D generalized strains and unknown warping functions. The unknown warping functions for each approximation can be obtained in terms of 2D generalized strains corresponding to the stationary points of the functionals, which are one-dimensional (1D) analyses through the thickness. Solutions for the warping functions can be obtained analytically as shown in Ref. [39] and Ref. [37]. After solving for the unknown warping functions, one can substitute them back into the energy functionals in Eq. 1 to obtain 2D energy functionals for 2D plate analysis. For example, for the zeroth-order approximation, the 2D plate model of VAPAS is of the form

$$\Pi_0 = \Pi_0(\epsilon_{11}, \epsilon_{12}, \epsilon_{22}, \kappa_{11}, \kappa_{12}, \kappa_{22}) \tag{3}$$

It should be noted that the energy functional for the zeroth-order approximation, Π_0, coincides to that of CLT but without invoking the Kirchhoff hypothesis and the transverse normal is flexible during deformation.

Higher-order approximations can be used to construct refined models. For example, the approximation through second order (h^2/l^2) should be used to handle transverse shear effects. However, there are two challenging issues associated with the second-order approximation:

- The energy functional asymptotically correct up through the second order is in terms of the CLT generalized strains *and their derivatives*. This form is not convenient for plate analysis because the boundary conditions cannot be readily associated with quantities normally specified on the boundary of plates.
- Only part of the second-order energy corresponds to transverse shear deformation, and no physical interpretation is known for the remaining terms.

VAPAS uses exact kinematical relations between derivatives of the generalized strains of CLT and the transverse shear strains along with equilibrium equations to meet these challenges. Minimization techniques are then applied to find the transverse shear energy that is closest to the asymptotically correct second-order energy. In other words, the loss of accuracy between the asymptotically correct model and a generalized Reissner-Mindlin model is minimized mathematically. For the purpose of establishing a direct connection be-

tween 2D Reissner-Mindlin plate finite element analysis, the through-thickness analysis is implemented using a 1D finite element discretization in the computer program VAPAS, which has direct connection with the plate/shell elements in commercial finite element packages and can be conveniently used by application-oriented engineers.

In comparison to most existing composite plate modeling approaches, VAPAS has several unique features:

- VAPAS adopts VAM to rigorously split the original geometrically-exact, nonlinear 3D problem into a linear, 1D, through-the-thickness analysis and a geometrically-exact, nonlinear, 2D, plate analysis. This novel feature allows the global plate analysis to be formulated exactly and intrinsically as a generalized 2D continuum over the reference plane and routes all the approximations into the through-the-thickness analysis, the accuracy of which is guaranteed to be the best by use of the VAM. The optimization procedure minimizes the loss of information in recasting the model to the generalized Reissner-Mindlin form.
- No kinematical assumptions are invoked in the derivation. All deformation of the normal line element is correctly described by the warping functions within the accuracy of the asymptotic approximation.
- VAPAS does not rely on integration of the 3D equilibrium equations through the thickness to obtain accurate distributions of transverse normal and shear strains and stresses.
- VAPAS exactly satisfies all continuity conditions, including those on both displacement and stress, at the interfaces as well as traction conditions on the top and bottom surfaces.
- The resulting plate/shell analysis is geometrically exact, far beyond von-Karman type nonlinearity commonly used in the literature, needed for highly flexible applications.

3 Considered Axiomatic Plate Theories: the Generalized Unified Formulation

3.1 Classification of the Theories

The main feature of the Generalized Unified Formulation (GUF) is that the descriptions of Layerwise Theories, Higher-order Shear Deformation Theories and Zig-Zag Theories of any combination of orders *do not show any formal differences* and can all be obtained from six invariant kernels. So, with just one theoretical model an infinite number of different approaches can be considered. For example, in the case of moderately thick plates a higher order theory

could be sufficient but for thick plates layerwise models may be required. With GUF the two approaches are formally identical because the kernels are invariant with respect to the type of theory.

In the present work the concepts of *type of theory* and *class of theories* are introduced. The following types of displacement-based theories are discussed. The first type is named as Advanced Higher-order Shear Deformation Theories (AHSDT). These theories are Equivalent Single Layer models because the displacement field is unique and independent of the number of layers. The effects of the transverse normal strain ε_{zz} are retained.
The second type of theories is named as Advanced Higher-order Shear Deformation Theories with Zig-Zag effects included (AHSDTZ). These theories are Equivalent Single Layer models and the so called Zig-Zag form of the displacements is taken into account by using Murakami's Zig-Zag Function (MZZF). The effects of the transverse normal strain ε_{zz} are included. The third type of theories is named Advanced LayerWise Theories (ALWT). These theories are the most accurate ones because all the displacements have a layerwise description. The effects of the transverse normal strain ε_{zz} are included as well. These models are necessary when local effects need to be described. The price is of course (in FEM applications) in higher computational time. An infinite number of theories which have a particular logic in the selection of the used orders of expansion is defined as *class of theories*. For example, the infinite layerwise theories which have the displacements u_x, u_y and u_z expanded along the thickness with a polynomial of order N are a class of theories. The infinite theories which have the in-plane displacements u_x and u_y expanded along the thickness with order N, the out of plane displacement expanded along the thickness with order $N-1$ are another class of theories.

3.2 Basic Idea and Theoretical Formulation

Both layerwise and Equivalent Single Layer models are axiomatic approaches if the unknowns are expanded along the thickness by using *a chosen* series of functions.
When the Principal of Virtual Displacements is used, the unknowns are the displacements u_x, u_y and u_z. When other variational statements are used the unknowns may also be all or some of the stresses and other quantities as well (multifield case).
The Generalized Unified Formulation is introduced here considering a generic layer k of a multilayered plate structure. This is the most general approach and the Equivalent Single Layer theories, which consider the displacement unknowns to be layer-independent, can be derived from this formulation with

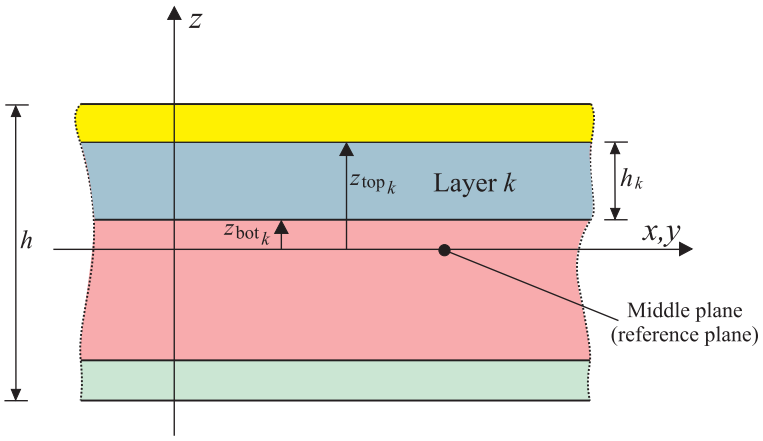

Fig. 1. Multilayered plate: notations and definitions.

some simple formal techniques[16]. Consider a theory denoted as Theory I, in which the displacement in x direction u_x^k has four Degrees of Freedom. Here by Degrees of Freedom it is intended the number of unknown quantities that are used to expand a variable. In the case under examination four Degrees of Freedom for the displacement u_x^k means that four unknowns are considered. Each unknown multiplies *a known function* of the thickness coordinate z. Where the origin of the coordinate z is measured is not important. However, from a practical point of view it is convenient to assume that the *middle plane* of the plate is also the plane with $z = 0$. This assumption does not imply that there is a symmetry with respect to the plane $z = 0$. The formulation is general.
For layer k the following relation holds: $z_{\text{bot}_k} \leq z \leq z_{\text{top}_k}$. z_{bot_k} is the global coordinate z of the bottom surface of layer k and z_{top_k} is the global coordinate z of the top surface of layer k (see Figure 1). $h_k = z_{\text{top}_k} - z_{\text{bot}_k}$ is the thickness of layer k and h is the thickness of the plate.
In the case of Theory I, u_x^k is expressed as follows:

$$u_x^k(x,y,z) = \overbrace{f_1^k(z)}^{\text{known}} \cdot \overbrace{u_{x_1}^k(x,y)}^{\text{unknown\#1}} + \overbrace{f_2^k(z)}^{\text{known}} \cdot \overbrace{u_{x_2}^k(x,y)}^{\text{unknown\#2}} + \underbrace{f_3^k(z)}_{\text{known}} \cdot \underbrace{u_{x_3}^k(x,y)}_{\text{unknown\#3}} + \underbrace{f_4^k(z)}_{\text{known}} \cdot \underbrace{u_{x_4}^k(x,y)}_{\text{unknown\#4}} \qquad z_{\text{bot}_k} \leq z \leq z_{\text{top}_k} \quad (4)$$

The functions $f_1^k(z)$, $f_2^k(z)$, $f_3^k(z)$ and $f_4^k(z)$ are *known* functions (axiomatic approach). These functions could be, for example, a series of trigonometric functions of the thickness coordinate z. Polynomials (or even better orthogonal polynomials) could be selected. In the most general case each layer has different functions. For example, $f_1^k(z) \neq f_1^{k+1}(z)$. The next *formal step* is to modify the notation.

The following functions are *defined*:

$$\begin{aligned} {}^{x}F_t^k(z) &= f_1^k(z) \qquad {}^{x}F_2^k(z) = f_2^k(z) \\ {}^{x}F_3^k(z) &= f_3^k(z) \qquad {}^{x}F_b^k(z) = f_4^k(z) \end{aligned} \tag{5}$$

The logic behind these definitions is the following. The *first* function $f_1^k(z)$ is defined as ${}^{x}F_t^k$. Notice the superscript x. It was added to clarify that the displacement in x direction, u_x^k, is under investigation. The subscript t identifies the quantities at the "top" of the plate and, therefore, are useful in the assembling of the stiffness matrices in the thickness direction (see Ref. [16]). The *last* function $f_4^k(z)$ is defined as ${}^{x}F_b^k$. Notice again the superscript x. The subscript b means "bottom" and, again, its utility is discussed in Ref. [16]. The intermediate functions $f_2^k(z)$ and $f_3^k(z)$ are defined simply as ${}^{x}F_2^k$ and ${}^{x}F_3^k$. To be consistent with the definitions of equation 5, the following unknown quantities are *defined*:

$$u_{x_t}^k(x,y) = u_{x_1}^k(x,y) \qquad u_{x_b}^k(x,y) = u_{x_4}^k(x,y) \tag{6}$$

Using the definitions reported in equations 5 and 6, equation 4 can be rewritten as

$$\begin{aligned} u_x^k(x,y,z) = {} & \overbrace{{}^{x}F_t^k(z)}^{\text{known}} \cdot \overbrace{u_{x_t}^k(x,y)}^{\text{unknown\#1}} + \overbrace{{}^{x}F_2^k(z)}^{\text{known}} \cdot \overbrace{u_{x_2}^k(x,y)}^{\text{unknown\#2}} \\ & + \underbrace{{}^{x}F_3^k(z)}_{\text{known}} \cdot \underbrace{u_{x_3}^k(x,y)}_{\text{unknown\#3}} + \underbrace{{}^{x}F_b^k(z)}_{\text{known}} \cdot \underbrace{u_{x_b}^k(x,y)}_{\text{unknown\#4}} \end{aligned} \qquad z_{\text{bot}_k} \leq z \leq z_{\text{top}_k} \tag{7}$$

It is supposed that each function of z is a polynomial. The order of the expansion is then 3 and indicated as $N_{u_x}^k$. Each layer has in general a different order. Thus, in general $N_{u_x}^k \neq N_{u_x}^{k+1}$. If the functions of z are not polynomials (for example, this is the case if trigonometric functions are used) then $N_{u_x}^k$ is just a parameter related to the number of terms or Degrees of Freedom used to describe the displacement u_x^k in the thickness direction. The expression representing the displacement u_x^k (see equation 7) can be put in a compact form typical of the Generalized Unified Formulation presented here. In particular it is possible to write:

$$u_x^k(x,y,z) = {}^{x}F_{\alpha_{u_x}}^k(z) \cdot u_{x\alpha_{u_x}}^k(x,y) \quad \alpha_{u_x} = t,l,b; \quad l = 2,...,N_{u_x}^k \tag{8}$$

where, in the example, $N_{u_x}^k = 3$. The thickness primary master index α has the subscript u_x. This subscript from now on will be called *slave index*. It is introduced to show that the displacement u_x is considered. An *infinite* number

of theories can be included in equation 8. It is in fact sufficient to change the value of $N_{u_x}^k$. It should be observed that *formally* there is no difference between two distinct theories (obtained by changing $N_{u_x}^k$). It is deduced that ∞^1 theories can be represented by equation 8.
The other displacements u_y^k and u_z^k can be treated in a similar fashion. The Generalized Unified Formulation for all the displacements is the following:

$$\begin{aligned}
u_x^k &= {}^xF_t u_{x_t}^k + {}^xF_l u_{x_l}^k + {}^xF_b u_{x_b}^k = {}^xF_{\alpha_{u_x}} u_{x\alpha_{u_x}}^k \quad \alpha_{u_x} = t, l, b; \quad l = 2, ..., N_{u_x} \\
u_y^k &= {}^yF_t u_{y_t}^k + {}^yF_m u_{y_m}^k + {}^yF_b u_{y_b}^k = {}^yF_{\alpha_{u_y}} u_{y\alpha_{u_y}}^k \quad \alpha_{u_y} = t, m, b; \; m = 2, ..., N_{u_y} \\
u_z^k &= {}^zF_t u_{z_t}^k + {}^zF_n u_{z_n}^k + {}^zF_b u_{z_b}^k = {}^zF_{\alpha_{u_z}} u_{z\alpha_{u_z}}^k \quad \alpha_{u_z} = t, n, b; \quad n = 2, ..., N_{u_z}
\end{aligned} \tag{9}$$

In equation 9, for simplicity it is assumed that the type of functions is the same for each layer and that the same number of terms is used for each layer. This assumption will make it possible to adopt the same Generalized Unified Formulation for all types of theories, and layerwise and equivalent single layer theories will *not* show formal differences. This concept means, for example, that if displacement u_y is approximated with five terms in a particular layer k then it will be approximated with five terms in *all* layers of the multilayered structure.
Each displacement variable can be expanded in ∞^1 combinations. In fact, it is sufficient to change the number of terms used for each variable. Since there are three variables (the displacements u_x, u_y and u_z), it is concluded that equation 9 includes ∞^3 different theories. In equation 9 the quantities are defined in a layerwise sense but it can be shown that the same concept is valid for the Equivalent Single Layer cases too (see Ref. [16]).
It can be shown that when a theory generated by using GUF has the orders of the expansions of all the displacements equal to each other, the results are numerically identical to the ones that can be obtained by using Carrera's Unified Formulation (see Ref. [11]). This is a logical consequence of the fact that GUF can be considered as an extension and generalization of CUF (see more details in Ref. [17]).

3.3 Acronyms Used to Identify a Generic Theory Obtained by Using GUF

Three types of displacement-based theories can be obtained. As stated above, the first type is named Advanced Higher-order Shear Deformation Theories (AHSDT). A AHSDT theory with orders of expansion N_{u_x}, N_{u_y} and N_{u_z} for the displacements u_x, u_y and u_z respectively, is denoted as $ED_{N_{u_x}N_{u_y}N_{u_z}}$. "E" stands for "Equivalent Single Layer" and "D" stands for "Displacement-based" theory.

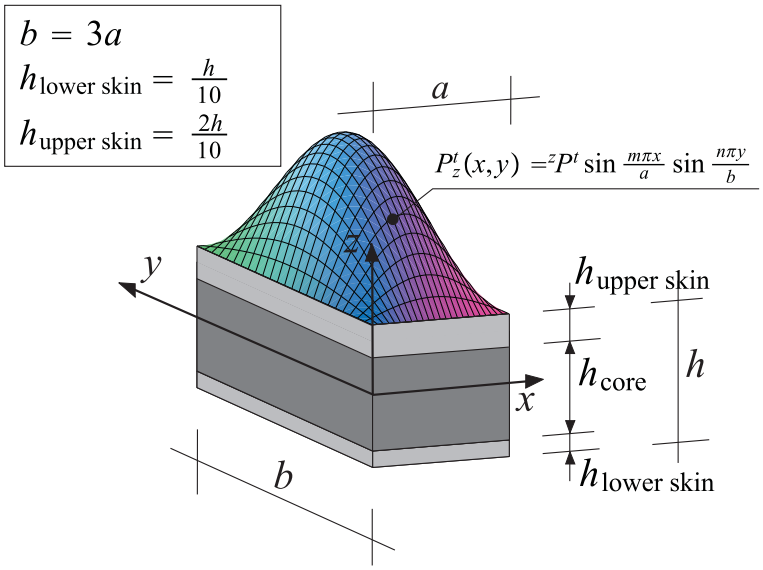

Fig. 2. Test Case 1. Geometry of the plate sandwich structure.

With similar logic, it is possible to define acronyms for the second type (Advanced Higher-order Shear Deformation Theories with Zig-Zag effects included (AHSDTZ)) and for the third type of theories (Advanced LayerWise Theories (ALWT)). The acronyms are $EDZ_{N_{ux}N_{uy}N_{uz}}$ and $LD_{N_{ux}N_{uy}N_{uz}}$ (more details can be found in Ref. [16]). For example, a AHSDTZ theory with cubic orders for all the displacements is indicated as EDZ_{333} whereas a ALWT theory with parabolic orders for all the displacements is indicated as LD_{222}.

4 Results

Two test cases are analyzed in this work.

4.1 Description of Test Case 1

Test case 1 is a sandwich plate (see Figure 2) made of two skins and a core [$h_{\text{lower skin}} = h/10$; $h_{\text{upper skin}} = 2h/10$; $h_{\text{core}} = (7/10)h$]. It is also $\frac{E_{\text{lower skin}}}{E_{\text{upper skin}}} = 5/4$. The plate is simply supported and the load is a sinusoidal pressure applied at the top surface of the plate ($m = n = 1$). Different Face-to-Core Stiffness Ratio (FCSR) are proposed here:

- Face-to-Core Stiffness Ratio $= FCSR = \frac{E_{\text{lower skin}}}{E_{\text{core}}} = 10^1$; $a/h = 4, 10, 100$
- Face-to-Core Stiffness Ratio $= FCSR = \frac{E_{\text{lower skin}}}{E_{\text{core}}} = 10^5$; $a/h = 4, 100$

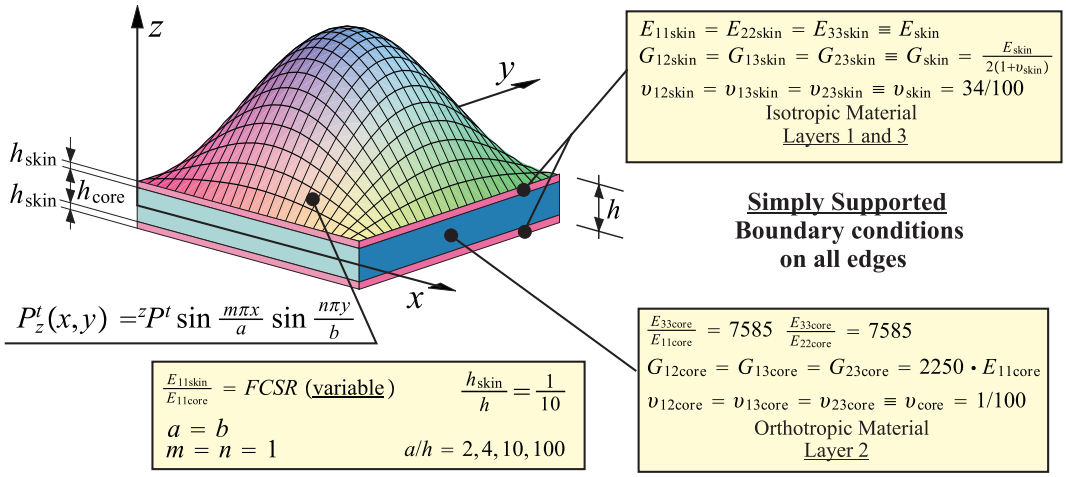

Fig. 3. Test Case 2 (see also [12])

As far as Poisson's ratio is concerned, the following values are used: $\upsilon_{\text{lower skin}} = \upsilon_{\text{upper skin}} = \upsilon_{\text{core}} = \upsilon = 0.34$. The middle plane of the plate is a rectangle with $b = 3a$. In this test case there is *no symmetry* with respect to the plane $z = 0$.

4.2 Description of Test Case 2

This test case is represented by a *symmetric* sandwich structure. The case has been taken from reference [12] and all the details can be obtained from Figure 3.

4.3 Test Case 1: Numerical Results and Discussion

The following non-dimensional quantities are introduced:

$$\begin{aligned}
&\widehat{u}_x = u_x \frac{E_{\text{core}}}{{}_zP^t h\left(\frac{a}{h}\right)^3}; \quad \widehat{u}_y = u_y \frac{E_{\text{core}}}{{}_zP^t h\left(\frac{a}{h}\right)^3}; \quad \widehat{u}_z = u_z \frac{100E_{\text{core}}}{{}_zP^t h\left(\frac{a}{h}\right)^4}; \\
&\widehat{\sigma}_{zx} = \frac{\sigma_{zx}}{{}_zP^t\left(\frac{a}{h}\right)}; \quad \widehat{\sigma}_{zy} = \frac{\sigma_{zy}}{{}_zP^t\left(\frac{a}{h}\right)}; \quad \widehat{\sigma}_{zz} = \frac{\sigma_{zz}}{{}_zP^t}; \\
&\widehat{\sigma}_{xx} = \frac{\sigma_{xx}}{{}_zP^t\left(\frac{a}{h}\right)^2}; \quad \widehat{\sigma}_{yy} = \frac{\sigma_{yy}}{{}_zP^t\left(\frac{a}{h}\right)^2}; \quad \widehat{\sigma}_{xy} = \frac{\sigma_{xy}}{{}_zP^t\left(\frac{a}{h}\right)^2};
\end{aligned} \tag{10}$$

All the results have been compared with the solution obtained by solving the "exact" problem [15]. The exact value is indicated with the terminology "elasticity" and is the reference value corresponding to the solution of the differential equations that govern the problem according to the three-dimensional elasticity theory. The details of this elasticity solution are here omitted for

brevity. The relative error $Err\%$ used in the tables is defined as follows:

$$Err\% = 100 \cdot \frac{\text{Result current theory} - \text{Result elasticity solution}}{\text{Result elasticity solution}} \tag{11}$$

Tables 1 and 2 compare a ALWT, AHSDT, AHSDTZ and VAPAS with VAPAS0 denoting the zeroth-order approximation of VAPAS according to Eq. 3. As shown in Table 1, VAPAS0 has a similar prediction for transverse deflection as ED_{111} for a thick plate ($a/h = 4$) for both $FCSR = 10$ and $FCSR = 10^5$. It is noted that ED_{111} is very similar to CLT with a flexible transverse normal. For thin plates with mild modulus contrast, VAPAS0 has an accuracy similar to higher-order theories without zigzag effects ($ED_{444}, ED_{555}, ED_{777}$). For thin plates with big modulus contrast ($FCSR = 10^5$), VAPAS0 has an accuracy similar to ED_{444}. VAPAS results for the deflection prediction are generally better than VAPAS0 and has an accuracy comparable to higher-order theories with zig-zag effects such as EDZ_{444} and higher. The only anomaly case is that for thick plates with the big modulus contrast, VAPAS results are not meaningful. This could be explained that VAPAS is not constructed for such an extreme case. Note in Eq. 2, only the geometrical small parameter h/a is used for the asymptotical expansion, yet for this extreme case, the modulus contrast is a much smaller parameter than h/a. Hence, it is suggested that VAPAS is not suitable for thick sandwich plates with huge modulus contrast. Note for the sandwich plate with $a/h = 100$ and $FCSR = 10^5$, VAPAS predicts reasonably well. Later we will use more examples to demonstrate that for moderate modulus contrast, VAPAS actually has a very good prediction. Similar observations can be made about the stress prediction as shown in Table 2. It is worthy to point out that VAPAS plate model only uses three DOFs for its zeroth-order approximation and five DOFs for its first-order approximation. The 2D plate element of VAPAS is the same as a FOSDT and is more efficient than all other theories listed in the tables. In other words, VAPAS presents a great compromise between the accuracy of the results and the number of DOFs. Tables 3-11 present a relatively thick sandwich plate with $FCSR = 10$. The out-of-plane stresses are not unknowns of the displaced-based theories based on GUF (this is not the case if a mixed variational theorem is used). Therefore, they can be calculated *a posteriori* by using Hooke's law or by integrating the equilibrium equations of the three-dimensional elasticity theory. The first approach is usually not satisfactory for ESL theories. Therefore, all the axiomatic results presented in this work report the transverse stresses calculated by integrating the equilibrium equations. In all cases it is possible to see that VAPAS has an accuracy comparable or superior to AHSDTZ. For this particular case we tested, VAPAS has a similar accuracy as, or for most cases better, than EDZ_{555} for displacement prediction and in-plane stress and transverse normal stress prediction and its accuracy is similar to LD_{222}. For transverse shear stresses, VAPAS predicts similar values as EDZ_{555}. It is worthy to note that VAPAS achieves these accurate predictions without integrat-

a/h	4		100		
		$\frac{E_{\text{lower skin}}}{E_{\text{core}}} \equiv FCSR = 10^1$			
$Elasticity$	3.01123	$Err.\%$	1.51021	$Err.\%$	DOF
LD_{111}	2.98058	(-1.02)	1.47242	(-2.50)	12
LD_{222}	3.00982	(-0.05)	1.51021	(0.00)	21
LD_{555}	3.01123	(0.00)	1.51021	(0.00)	48
ED_{111}	1.58218	(-47.5)	1.10845	(-26.6)	6
ED_{444}	2.79960	(-7.03)	1.50989	(-0.02)	15
ED_{555}	2.84978	(-5.36)	1.50996	(-0.02)	18
ED_{777}	2.86875	(-4.73)	1.50999	(-0.01)	24
EDZ_{111}	2.34412	(-22.2)	1.15866	(-23.3)	9
EDZ_{444}	2.97886	(-1.07)	1.51017	(0.00)	18
EDZ_{555}	2.98737	(-0.79)	1.51018	(0.00)	21
EDZ_{777}	2.99670	(-0.48)	1.51019	(0.00)	27
$VAPAS_0$	1.5136	(-49.7)	1.50788	(-0.15)	3
$VAPAS$	3.0198	(0.28)	1.5102	(0.00)	5
		$\frac{E_{\text{lower skin}}}{E_{\text{core}}} \equiv FCSR = 10^5$			
$Elasticity$	$1.31593 \cdot 10^{-02}$	$Err.\%$	$2.08948 \cdot 10^{-03}$	$Err.\%$	
LD_{111}	$9.79008 \cdot 10^{-03}$	(-25.6)	$1.96509 \cdot 10^{-03}$	(-5.95)	12
LD_{222}	$1.31471 \cdot 10^{-02}$	(-0.09)	$2.08948 \cdot 10^{-03}$	(0.00)	21
LD_{555}	$1.31593 \cdot 10^{-02}$	(0.00)	$2.08949 \cdot 10^{-03}$	(0.00)	48
ED_{111}	$1.79831 \cdot 10^{-04}$	(-98.6)	$1.19941 \cdot 10^{-04}$	(-94.3)	6
ED_{444}	$1.16851 \cdot 10^{-03}$	(-91.1)	$1.64835 \cdot 10^{-04}$	(-92.1)	15
ED_{555}	$4.29224 \cdot 10^{-03}$	(-67.4)	$1.73120 \cdot 10^{-04}$	(-91.7)	18
ED_{777}	$1.08119 \cdot 10^{-02}$	(-17.8)	$2.96304 \cdot 10^{-04}$	(-85.8)	24
EDZ_{111}	$8.36735 \cdot 10^{-04}$	(-93.6)	$1.63329 \cdot 10^{-04}$	(-92.2)	9
EDZ_{444}	$1.26288 \cdot 10^{-02}$	(-4.03)	$1.16305 \cdot 10^{-03}$	(-44.3)	18
EDZ_{555}	$1.30409 \cdot 10^{-02}$	(-0.90)	$1.78411 \cdot 10^{-03}$	(-14.6)	21
EDZ_{777}	$1.31363 \cdot 10^{-02}$	(-0.17)	$2.02060 \cdot 10^{-03}$	(-3.30)	27
$VAPAS_0$	$1.6421 \cdot 10^{-04}$	(-98.7)	$1.6314 \cdot 10^{-04}$	(-92.2)	3
$VAPAS$	1.49076	(> 100)	$2.4667 \cdot 10^{-03}$	(18.0)	5

Table 1
Test Case 1. Comparison of various theories to evaluate the transverse displacements amplitude (center plate deflection) $\widehat{u}_z = u_z \frac{100 E_{\text{core}}}{{}_z P^t h \left(\frac{a}{h}\right)^4}$ in $z = z_{\text{bottom}}^{\text{upper skin}} = \frac{3}{10}h$, $x = a/2$, $y = b/2$.

a/h	4	$Err.$	100	$Err.$	
		$\frac{E_{\text{lower skin}}}{E_{\text{core}}} \equiv FCSR = 10^1$			
$Elasticity$	0.32168	$Err.\%$	0.33176	$Err.\%$	DOF
LD_{111}	0.31730	(-1.36)	0.32345	(-2.50)	12
LD_{222}	0.32142	(-0.08)	0.33176	(0.00)	21
LD_{555}	0.32168	(0.00)	0.33176	(0.00)	48
ED_{111}	0.33178	$(+3.14)$	0.33178	$(+0.01)$	6
ED_{444}	0.33240	$(+3.33)$	0.33178	$(+0.01)$	15
ED_{555}	0.32884	$(+2.23)$	0.33178	$(+0.01)$	18
ED_{777}	0.32707	$(+1.68)$	0.33177	(0.00)	24
EDZ_{111}	0.34184	$(+6.27)$	0.34497	$(+3.98)$	9
EDZ_{444}	0.32913	$(+2.32)$	0.33178	$(+0.01)$	18
EDZ_{555}	0.32755	$(+1.82)$	0.33177	(0.00)	21
EDZ_{777}	0.32530	$(+1.12)$	0.33177	$(+0.00)$	27
$VAPAS_0$	0.33178	$(+3.14)$	0.33178	$(+0.01)$	3
$VAPAS$	0.31037	(-3.5)	0.33175	$(+0.00)$	5
		$\frac{E_{\text{lower skin}}}{E_{\text{core}}} \equiv FCSR = 10^5$			
$Elasticity$	$5.40842 \cdot 10^{-04}$	$Err.\%$	0.27797	$Err.\%$	
LD_{111}	$1.05700 \cdot 10^{-04}$	(-80.5)	0.26143	(-5.95)	12
LD_{222}	$5.37740 \cdot 10^{-04}$	(-0.57)	0.27797	(0.00)	21
LD_{555}	$5.40842 \cdot 10^{-04}$	(0.00)	0.27797	(0.00)	48
ED_{111}	0.33242	(> 100)	0.33242	$(+19.6)$	6
ED_{444}	0.30529	(> 100)	0.33238	$(+16.6)$	15
ED_{555}	0.21639	(> 100)	0.33214	$(+19.5)$	18
ED_{777}	$3.96907 \cdot 10^{-02}$	(> 100)	0.32865	$(+18.2)$	24
EDZ_{111}	0.30971	(> 100)	0.33077	$(+19.0)$	9
EDZ_{444}	$6.84336 \cdot 10^{-03}$	(> 100)	0.30392	$(+9.34)$	18
EDZ_{555}	$1.87520 \cdot 10^{-03}$	(> 100)	0.28655	$(+3.09)$	21
EDZ_{777}	$8.02443 \cdot 10^{-04}$	$(+48.4)$	0.27994	$(+0.71)$	27
$VAPAS_0$	0.33242	(> 100)	0.33242	$(+19.6)$	3
$VAPAS$	0.30592	(> 100)	0.33238	$(+16.6)$	5

Table 2
Test Case 1. Comparison of various theories to evaluate the transverse shear stress $\widehat{\sigma}_{zx} = \frac{\sigma_{zx}}{{}_zP^t\left(\frac{a}{h}\right)}$ in $z = z^{\text{upper skin}}_{\text{bottom}} = \frac{3}{10}h$, $x = 0$, $y = b/2$. The indefinite equilibrium equations have been integrated along the thickness except VAPAS0 and VAPAS.

ing the 3D equilibrium equations. If integration through the thickness is not used to obtain such values in the displacement-based GUT theories, EDZ_{555} will be expected to be worse than VAPAS results. For moderate $FCSR$ values and thick plates ($a/h = 4$, see Figures 4-7, VAPAS presents results that can be comparable of the results obtained by using the axiomatic zig-zag theory EDZ_{777}. This is particularly evident in Figure 7. However, the VAPAS plate model only requires five DOFs, which is only less than 20% of the computational cost one would need for EDZ_{777} (27 DOFs). It is also noted, VAPAS plate model remains the same as the well-known Reissner-Mindlin elements universally available in all commercial finite element packages.

The Equivalent Single Layer and Layerwise axiomatic theories presented in this paper and a virtually infinite number of other theories can be implemented in a single FEM code based on the Generalized Unified Formulation. Accuracy and CPU time requirements can be easily met with an appropriate selection of the type of theory and the orders used in the expansions of the displacements.

a/h	10		
	$\frac{E_{\text{lower skin}}}{E_{\text{core}}} \equiv FCSR = 10^1$		
$Elasticity$	$-0.11087 \cdot 10^{-01}$	$Err.\%$	DOF
LD_{111}	$-0.10800 \cdot 10^{-01}$	(-2.59)	12
LD_{222}	$-0.11085 \cdot 10^{-01}$	(-0.01)	21
LD_{333}	$-0.11087 \cdot 10^{-01}$	(-0.00)	30
LD_{444}	$-0.11087 \cdot 10^{-01}$	(-0.00)	39
ED_{111}	$-0.08627 \cdot 10^{-01}$	(-22.2)	6
ED_{222}	$-0.11736 \cdot 10^{-01}$	$(+5.85)$	9
ED_{333}	$-0.11358 \cdot 10^{-01}$	$(+2.45)$	12
ED_{444}	$-0.11316 \cdot 10^{-01}$	$(+2.07)$	15
ED_{555}	$-0.11242 \cdot 10^{-01}$	$(+1.40)$	18
EDZ_{111}	$-0.08696 \cdot 10^{-01}$	(-21.6)	9
EDZ_{222}	$-0.11161 \cdot 10^{-01}$	$(+0.67)$	12
EDZ_{333}	$-0.11166 \cdot 10^{-01}$	$(+0.71)$	15
EDZ_{444}	$-0.11164 \cdot 10^{-01}$	$(+0.69)$	18
EDZ_{555}	$-0.11146 \cdot 10^{-01}$	$(+0.53)$	21
$VAPAS$	$-0.111009 \cdot 10^{-01}$	$(+0.13)$	5

Table 3
Test Case 1. Comparison of various theories to evaluate the in-plane displacement $\widehat{u}_x = u_x \frac{E_{\text{core}}}{{}^zP^t h \left(\frac{a}{h}\right)^3}$ in $z = z^{\text{upper skin}}_{\text{bottom}} = \frac{3}{10}h$, $x = 0$, $y = b/2$.

4.4 Test Case 2: Numerical Results and Discussion

The dimensionless displacements used for this study are defined as

$$\widehat{u}_x = u_x \frac{E_{\text{skin}}}{{}^zP^t h \left(\frac{a}{h}\right)^3}; \quad \widehat{u}_z = u_z \frac{100 E_{\text{skin}}}{{}^zP^t h \left(\frac{a}{h}\right)^4} \tag{12}$$

Notice the formal difference with the dimensionless quantities introduced in test case 1: here the elastic modulus used for the non-dimensional quantities is the elastic modulus of the skin and not the one of the core. The results are compared against the elasticity solution (see [15] and [17]). Tables 12, 13, 14, and 15 report some results obtained in reference [12] for thick, moderately thick and thin sandwich structures. The available results have been enriched with the new case of $a/h = 2$ and with the elasticity solution. The findings of

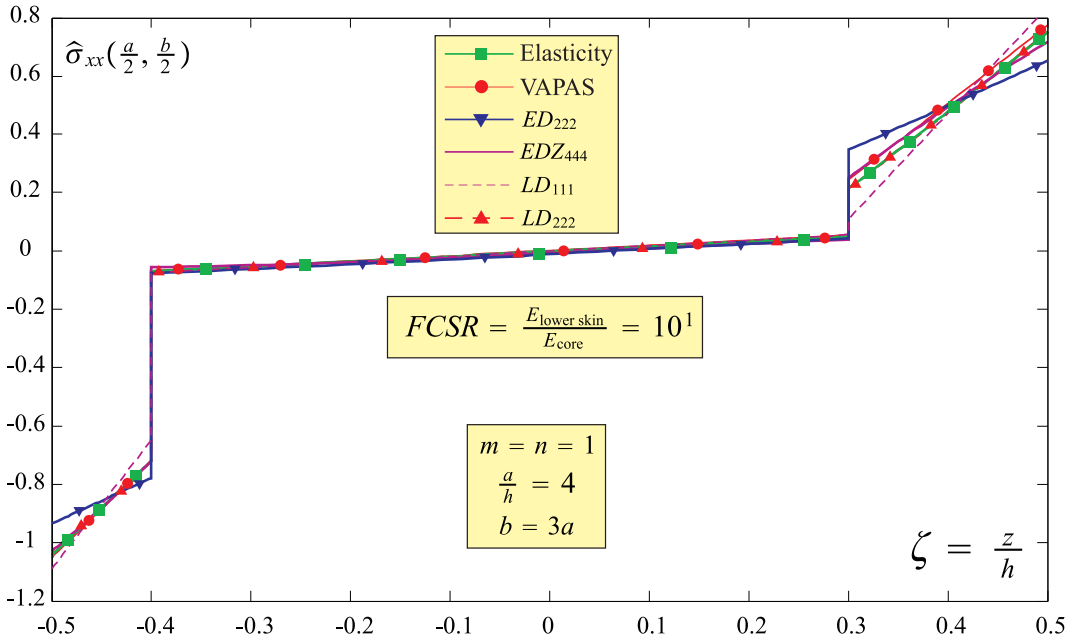

Fig. 4. Test Case 1. Comparison of various theories to evaluate the in-plane normal stress $\widehat{\sigma}_{xx} = \frac{\sigma_{xx}}{{}_zP^t\left(\frac{a}{h}\right)^2}$ in $x = a/2$, $y = b/2$. Note that this stress is not a continuous function on the thickness direction. Hooke's law has been used.

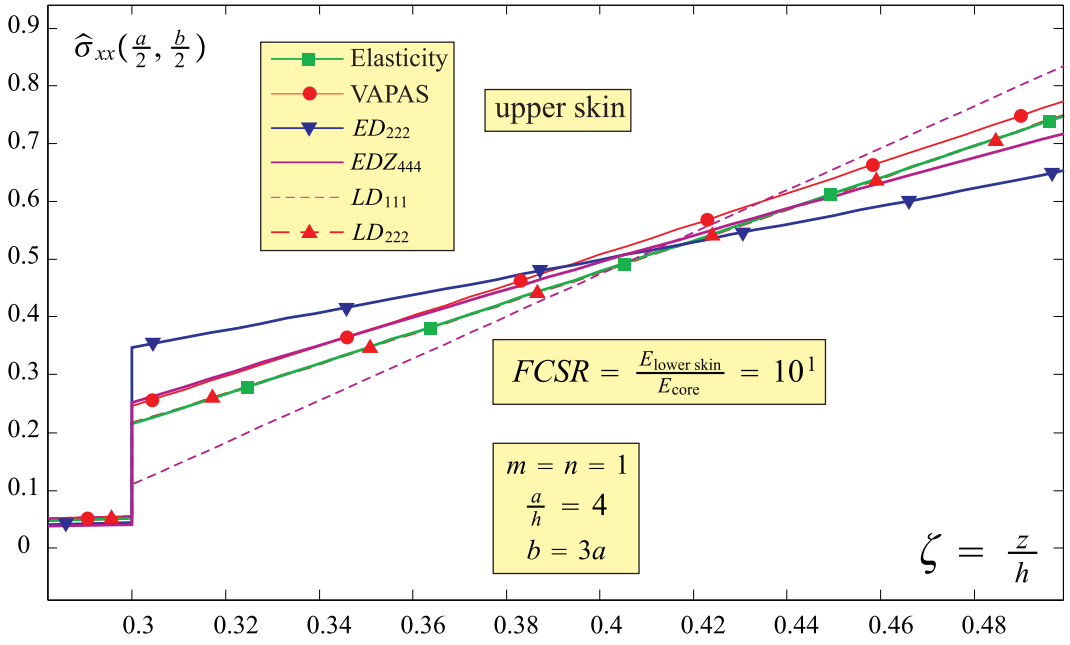

Fig. 5. Test Case 1. Comparison of various theories to evaluate the in-plane normal stress $\widehat{\sigma}_{xx} = \frac{\sigma_{xx}}{{}_zP^t\left(\frac{a}{h}\right)^2}$ in $x = a/2$, $y = b/2$ (upper-skin). Hooke's law has been used.

a/h	10		
	$\frac{E_{\text{lower skin}}}{E_{\text{core}}} \equiv FCSR = 10^1$		
$Elasticity$	$-0.36956 \cdot 10^{-02}$	$Err.\%$	DOF
LD_{111}	$-0.36000 \cdot 10^{-02}$	(-2.59)	12
LD_{222}	$-0.36952 \cdot 10^{-02}$	(-0.01)	21
LD_{333}	$-0.36956 \cdot 10^{-02}$	(-0.00)	30
LD_{444}	$-0.36956 \cdot 10^{-02}$	(-0.00)	39
ED_{111}	$-0.28757 \cdot 10^{-02}$	(-22.2)	6
ED_{222}	$-0.39120 \cdot 10^{-02}$	$(+5.85)$	9
ED_{333}	$-0.37860 \cdot 10^{-02}$	$(+2.45)$	12
ED_{444}	$-0.37721 \cdot 10^{-02}$	$(+2.07)$	15
ED_{555}	$-0.37473 \cdot 10^{-02}$	$(+1.40)$	18
EDZ_{111}	$-0.28986 \cdot 10^{-02}$	(-21.6)	9
EDZ_{222}	$-0.37204 \cdot 10^{-02}$	$(+0.67)$	12
EDZ_{333}	$-0.37220 \cdot 10^{-02}$	$(+0.71)$	15
EDZ_{444}	$-0.37213 \cdot 10^{-02}$	$(+0.69)$	18
EDZ_{555}	$-0.37153 \cdot 10^{-02}$	$(+0.53)$	21
$VAPAS$	$-0.37003 \cdot 10^{-02}$	$(+0.13)$	5

Table 4
Test Case 1. Comparison of various theories to evaluate the in-plane displacement $\widehat{u}_y = u_y \frac{E_{\text{core}}}{zP^t h\left(\frac{a}{h}\right)^3}$ in $z = z^{\text{upper skin}}_{\text{bottom}} = \frac{3}{10}h$, $x = a/2$, $y = 0$.

reference [12] have been confirmed: the equivalent single layer theories are not indicated to analyze very challenging sandwich structures especially if the face-to-core stiffness ratio is very high and the aspect ratio is small (thick plates). This result is also confirmed in figures 8, 9, and 10. In particular, it is clear from Figure 10 (which presents several AHSDTZ theories) that even zig zag theories with considerably high order for the expansion of the variables present significant error especially in the core region. As previously discussed in Test Case 1, VAPAS provides excellent results for moderate FCSRs. Specifically for this example, VAPAS predicts accurately for FCSR=73 and 7.3×10^4. VAPAS can provide meaningful results for very large FCSR for only if the aspect ratio is very large, for example FCSR=7.3×10^6 and $a/h = 10, 100$, and FCSR=7.3×10^8 and $a/h = 100$. If FCSR becomes larger and the plate is relatively thick, VAPAS becomes not predictive, for example when FCSR=7.3×10^6 and $a/h = 2, 4$, and FCSR=7.3×10^8 and $a/h = 2, 4, 10$. This example again suggests that VAPAS presents superior performances with respect to the classical equivalent

a/h	10		
	$\frac{E_{\text{lower skin}}}{E_{\text{core}}} \equiv FCSR = 10^1$		
$Elasticity$	1.74265	$Err.\%$	DOF
LD_{111}	1.70908	(-1.93)	12
LD_{222}	1.74247	(-0.01)	21
LD_{333}	1.74265	(-0.00)	30
LD_{444}	1.74265	(-0.00)	39
ED_{111}	1.18207	(-32.2)	6
ED_{222}	1.58561	(-9.01)	9
ED_{333}	1.70006	(-2.44)	12
ED_{444}	1.71032	(-1.85)	15
ED_{555}	1.71796	(-1.42)	18
EDZ_{111}	1.34741	(-22.7)	9
EDZ_{222}	1.73669	(-0.34)	12
EDZ_{333}	1.73805	(-0.26)	15
EDZ_{444}	1.73836	(-0.25)	18
EDZ_{555}	1.73938	(-0.19)	21
$VAPAS$	1.74265	$(+0.00)$	5

Table 5
Test Case 1. Comparison of various theories to evaluate the transverse displacements amplitude (center plate deflection) $\widehat{u}_z = u_z \frac{100 E_{\text{core}}}{{}_z P^t h \left(\frac{a}{h}\right)^4}$ in $z = z_{\text{bottom}}^{\text{upper skin}} = \frac{3}{10}h$, $x = a/2$, $y = b/2$.

single-layer zig-zag models for regular composite laminates when FCSR is moderate and the plate is not too thick. For thick sandwich plate with large FCSR, other small parameter considering both FCSR and the aspect ratio should be considered as suggested in Ref. [6].

a/h	10		
	$\frac{E_{\text{lower skin}}}{E_{\text{core}}} \equiv FCSR = 10^1$		
$Elasticity$	0.33146	$Err.\%$	DOF
LD_{111}	0.26290	(-20.7)	12
LD_{222}	0.33169	$(+0.07)$	21
LD_{333}	0.33144	(-0.00)	30
LD_{444}	0.33146	$(+0.00)$	39
ED_{111}	0.36049	$(+8.76)$	6
ED_{222}	0.35272	$(+6.41)$	9
ED_{333}	0.34357	$(+3.65)$	12
ED_{444}	0.34649	$(+4.54)$	15
ED_{555}	0.34260	$(+3.36)$	18
EDZ_{111}	0.35807	$(+8.03)$	9
EDZ_{222}	0.32847	(-0.90)	12
EDZ_{333}	0.33559	$(+1.25)$	15
EDZ_{444}	0.33753	$(+1.83)$	18
EDZ_{555}	0.33678	$(+1.60)$	21
$VAPAS$	0.33364	$(+0.66)$	5

Table 6
Test Case 1. Comparison of various theories to evaluate the in-plane normal stress $\widehat{\sigma}_{xx} = \frac{\sigma_{xx}}{{}_zP^t\left(\frac{a}{h}\right)^2}$ in $z = z_{\text{bottom}}^{\text{upper skin}} = \frac{3}{10}h$, $x = a/2$, $y = b/2$. Note that this stress is not a continuous function on the thickness direction. Hooke's law has been used.

a/h	10		
	$\frac{E_{\text{lower skin}}}{E_{\text{core}}} \equiv FCSR = 10^1$		
$Elasticity$	0.14662	$Err.\%$	DOF
LD_{111}	0.08285	(-43.5)	12
LD_{222}	0.14688	$(+0.17)$	21
LD_{333}	0.14660	(-0.01)	30
LD_{444}	0.14662	$(+0.00)$	39
ED_{111}	0.21666	$(+47.8)$	6
ED_{222}	0.15706	$(+7.12)$	9
ED_{333}	0.15421	$(+5.18)$	12
ED_{444}	0.15783	$(+7.64)$	15
ED_{555}	0.15518	$(+5.84)$	18
EDZ_{111}	0.21309	$(+45.3)$	9
EDZ_{222}	0.14239	(-2.88)	12
EDZ_{333}	0.14943	$(+1.92)$	15
EDZ_{444}	0.15141	$(+3.27)$	18
EDZ_{555}	0.15095	$(+2.95)$	21
$VAPAS$	0.14758	$(+0.65)$	5

Table 7
Test Case 1. Comparison of various theories to evaluate the in-plane normal stress $\widehat{\sigma}_{yy} = \frac{\sigma_{yy}}{{}_zP^t\left(\frac{a}{h}\right)^2}$ in $z = z_{\text{bottom}}^{\text{upper skin}} = \frac{3}{10}h$, $x = a/2$, $y = b/2$. Note that this stress is not a continuous function on the thickness direction. Hooke's law has been used.

a/h	10		
	$\frac{E_{\text{lower skin}}}{E_{\text{core}}} \equiv FCSR = 10^1$		
$Elasticity$	$-0.69314 \cdot 10^{-01}$	$Err.\%$	DOF
LD_{111}	$-0.67520 \cdot 10^{-01}$	(-2.59)	12
LD_{222}	$-0.69305 \cdot 10^{-01}$	(-0.01)	21
LD_{333}	$-0.69314 \cdot 10^{-01}$	(-0.00)	30
LD_{444}	$-0.69314 \cdot 10^{-01}$	(-0.00)	39
ED_{111}	$-0.53936 \cdot 10^{-01}$	(-22.2)	6
ED_{222}	$-0.73372 \cdot 10^{-01}$	$(+5.85)$	9
ED_{333}	$-0.71010 \cdot 10^{-01}$	$(+2.45)$	12
ED_{444}	$-0.70749 \cdot 10^{-01}$	$(+2.07)$	15
ED_{555}	$-0.70283 \cdot 10^{-01}$	$(+1.40)$	18
EDZ_{111}	$-0.54366 \cdot 10^{-01}$	(-21.6)	9
EDZ_{222}	$-0.69779 \cdot 10^{-01}$	$(+0.67)$	12
EDZ_{333}	$-0.69808 \cdot 10^{-01}$	$(+0.71)$	15
EDZ_{444}	$-0.69795 \cdot 10^{-01}$	$(+0.69)$	18
EDZ_{555}	$-0.69684 \cdot 10^{-01}$	$(+0.53)$	21
$VAPAS$	$-0.69775 \cdot 10^{-01}$	$(+0.67)$	5

Table 8
Test Case 1. Comparison of various theories to evaluate the in-plane shear stress $\widehat{\sigma}_{xy} = \frac{\sigma_{xy}}{{}_zP^t\left(\frac{a}{h}\right)^2}$ in $z = z^{\text{upper skin}}_{\text{bottom}} = \frac{3}{10}h$, $x = 0$, $y = 0$. Note that this stress is not a continuous function on the thickness direction. Hooke's law has been used.

a/h	10		
	$\frac{E_{\text{lower skin}}}{E_{\text{core}}} \equiv FCSR = 10^1$		
$Elasticity$	0.32998	$Err.\%$	DOF
LD_{111}	0.32242	(-2.29)	12
LD_{222}	0.32994	(-0.01)	21
LD_{333}	0.32998	(-0.00)	30
LD_{444}	0.32998	(-0.00)	39
ED_{111}	0.33178	$(+0.55)$	6
ED_{222}	0.33210	$(+0.64)$	9
ED_{333}	0.33081	$(+0.25)$	12
ED_{444}	0.33178	$(+0.54)$	15
ED_{555}	0.33117	$(+0.36)$	18
EDZ_{111}	0.34444	$(+4.38)$	9
EDZ_{222}	0.33154	$(+0.47)$	12
EDZ_{333}	0.33140	$(+0.43)$	15
EDZ_{444}	0.33124	$(+0.38)$	18
EDZ_{555}	0.33096	$(+0.30)$	21
$VAPAS$	0.32836	(-0.50)	5

Table 9
Test Case 1. Comparison of various theories to evaluate the transverse shear stress $\widehat{\sigma}_{zx} = \frac{\sigma_{zx}}{{}_zP^t\left(\frac{a}{h}\right)}$ in $z = z^{\text{upper skin}}_{\text{bottom}} = \frac{3}{10}h$, $x = 0$, $y = b/2$. The indefinite equilibrium equations have been integrated along the thickness for all the theories except VAPAS.

a/h	10		
	$\frac{E_{\text{lower skin}}}{E_{\text{core}}} \equiv FCSR = 10^1$		
$Elasticity$	0.10999	$Err.\%$	DOF
LD_{111}	0.10747	(-2.29)	12
LD_{222}	0.10998	(-0.01)	21
LD_{333}	0.10999	(-0.00)	30
LD_{444}	0.10999	(-0.00)	39
ED_{111}	0.11059	$(+0.55)$	6
ED_{222}	0.11070	$(+0.64)$	9
ED_{333}	0.11027	$(+0.25)$	12
ED_{444}	0.11059	$(+0.54)$	15
ED_{555}	0.11039	$(+0.36)$	18
EDZ_{111}	0.11481	$(+4.38)$	9
EDZ_{222}	0.11051	$(+0.47)$	12
EDZ_{333}	0.11047	$(+0.43)$	15
EDZ_{444}	0.11041	$(+0.38)$	18
EDZ_{555}	0.11032	$(+0.30)$	21
$VAPAS$	0.10945	(-0.49)	5

Table 10
Test Case 1. Comparison of various theories to evaluate the transverse shear stress $\widehat{\sigma}_{zy} = \frac{\sigma_{zy}}{{}_zP^t\left(\frac{a}{h}\right)}$ in $z = z^{\text{upper skin}}_{\text{bottom}} = \frac{3}{10}h$, $x = a/2$, $y = 0$. The indefinite equilibrium equations have been integrated along the thickness for all the theories except VAPAS.

a/h	10		
	$\frac{E_{\text{lower skin}}}{E_{\text{core}}} \equiv FCSR = 10^1$		
$Elasticity$	0.87231	$Err.\%$	DOF
LD_{111}	0.87081	(-0.17)	12
LD_{222}	0.87233	$(+0.00)$	21
LD_{333}	0.87231	$(+0.00)$	30
LD_{444}	0.87231	(-0.00)	39
ED_{111}	0.51236	(-41.3)	6
ED_{222}	0.58831	(-32.6)	9
ED_{333}	0.77221	(-11.5)	12
ED_{444}	0.78478	$(-10.0$	15
ED_{555}	0.81517	(-6.55)	18
EDZ_{111}	0.51803	(-40.6)	9
EDZ_{222}	0.83586	(-4.18)	12
EDZ_{333}	0.83769	(-3.97)	15
EDZ_{444}	0.83847	(-3.88)	18
EDZ_{555}	0.84631	(-2.98)	21
$VAPAS$	0.87354	$(+0.14)$	5

Table 11
Test Case 1. Comparison of various theories to evaluate the transverse normal stress $\widehat{\sigma}_{zz} = \frac{\sigma_{zz}}{{}_zP^t}$ in $z = z_{\text{bottom}}^{\text{upper skin}} = \frac{3}{10}h$, $x = a/2$, $y = b/2$. The indefinite equilibrium equations have been integrated along the thickness for all the theories except VAPAS.

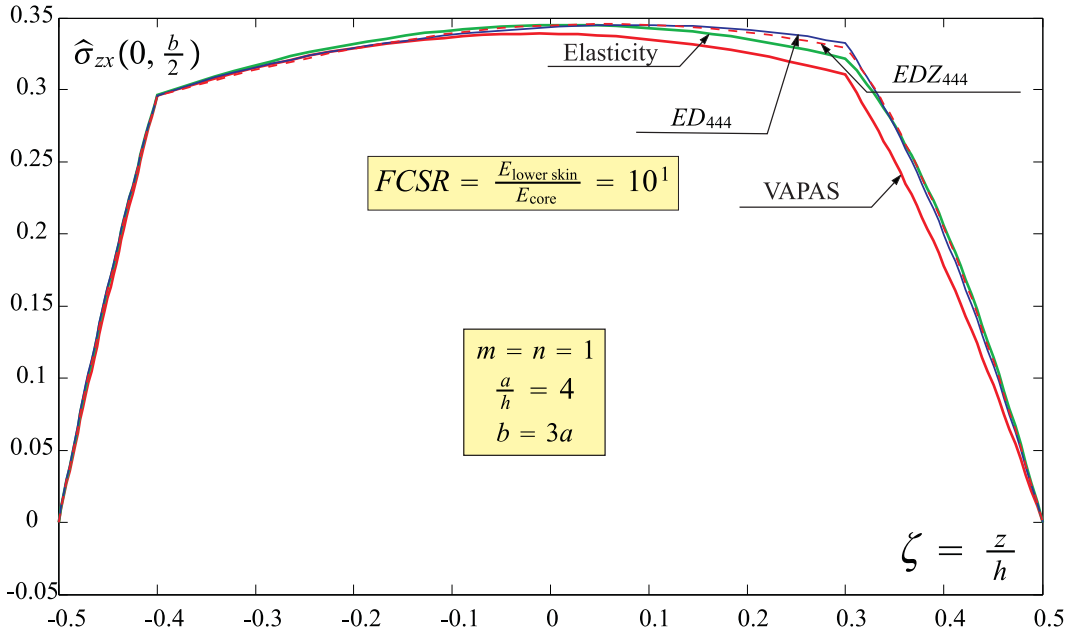

Fig. 6. Test Case 1. Comparison of various theories to evaluate the transverse shear stress $\widehat{\sigma}_{zx} = \frac{\sigma_{zx}}{{}^{z}P^{t}\left(\frac{a}{h}\right)}$ in $x = 0$, $y = b/2$. The indefinite equilibrium equations have been integrated along the thickness.

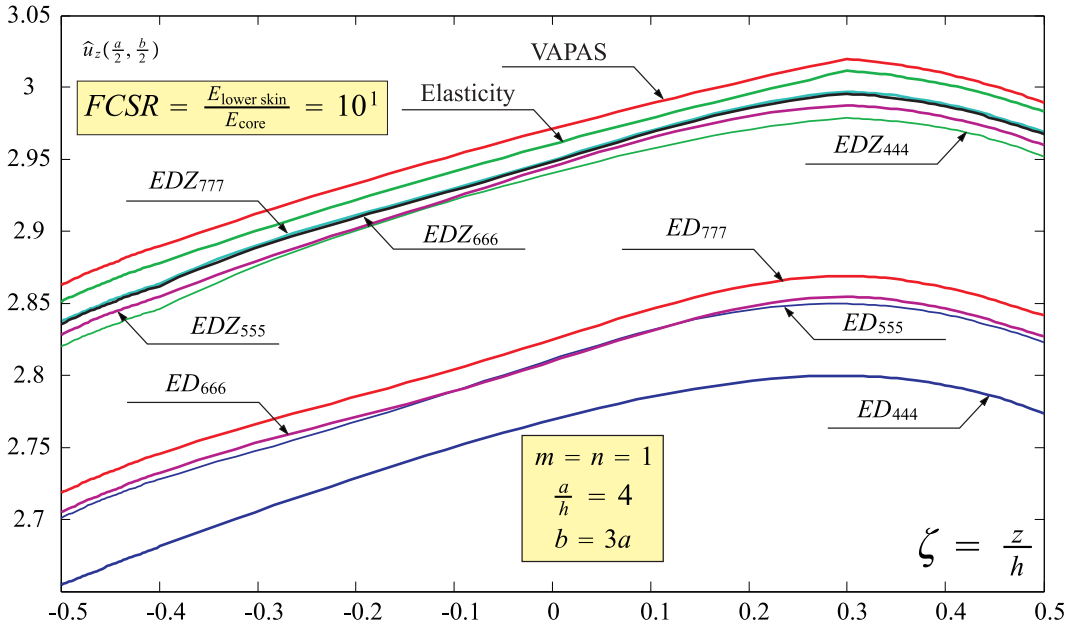

Fig. 7. Test Case 1. Comparison of various theories to evaluate the transverse displacements amplitude (center plate deflection) $\widehat{u}_z = u_z \frac{100 E_{\text{core}}}{{}^{z}P^{t} h \left(\frac{a}{h}\right)^4}$ in $x = a/2$, $y = b/2$.

a/h	2		4		10		100	
			$\frac{E_{11\,\text{skin}}}{E_{11\,\text{core}}} \equiv FCSR = 7.3 \times 10^1$					
Elasticity	0.227330	$Err\%$	0.198251	$Err\%$	0.190084	$Err\%$	0.188542	$Err\%$
$LM4$ [12]	NA	NA	0.1982	-0.03	0.1901	$+0.01$	0.1885	-0.02
$ED4$ [12]	NA	NA	NA	$\|1.61\|^\dagger$	NA	$\|0.79\|^\dagger$	NA	$\|1.22\|^\dagger$
$EMZC3$[12]	NA	NA	NA	$\|1.66\|^\dagger$	NA	$\|0.74\|^\dagger$	NA	$\|1.17\|^\dagger$
$LD1$ [12]	NA	NA	NA	$\|1.06\|^\dagger$	NA	$\|0.16\|^\dagger$	NA	$\|0.05\|^\dagger$
$LD4$ [12]	NA	NA	NA	$\|0.00\|^\dagger$	NA	$\|0.00\|^\dagger$	NA	$\|0.00\|^\dagger$
EDZ_{555}	0.246804	$+8.57$	0.201527	$+1.65$	0.188663	-0.75	0.186228	-1.23
LD_{222}	0.219334	-3.52	0.195992	-1.14	0.189710	-0.20	0.188538	-0.00
LD_{555}	0.227331	$+0.00$	0.198251	$+0.00$	0.190084	$+0.00$	0.188542	$+0.00$
$VAPAS$	0.191717	-15.67	0.192759	-2.77	0.189362	-0.38	0.188535	-0.00

Table 12
Test Case 2. $\frac{E_{11\,\text{skin}}}{E_{11\,\text{core}}} \equiv FCSR = 7.3 \times 10^1$. Comparison of various theories to evaluate the transverse displacements amplitude (center plate deflection) $\widehat{u}_z = u_z \frac{100 E_{22\,\text{skin}}}{{}_zP^t h \left(\frac{a}{h}\right)^4}$ in $x = a/2$, $y = b/2$, $z = 0$.
†In Reference [12] the percentage error $Err\%$ is calculated with respect to the $LM4$ theory. In reference [12] it was not specified the formula used for the percentage error. Therefore, in this table the absolute value is used for the errors reported in reference [12]. The present error evaluations are calculated with respect to the present elasticity solution (see equation 11).

a/h	2		4		10		100	
				$\frac{E_{11\,\text{skin}}}{E_{11\,\text{core}}} \equiv FCSR = 7.3 \times 10^4$				
Elasticity	45.6531	$Err\%$	15.4835	$Err\%$	7.03601	$Err\%$	5.44237	$Err\%$
$LM4$ [12]	NA	NA	15.483	-0.00	7.0360	-0.00	5.4424	$+0.00$
$ED4$ [12]	NA	NA	NA	$\|7.45\|^\dagger$	NA	$\|3.70\|^\dagger$	NA	$\|1.58\|^\dagger$
$EMZC3$[12]	NA	NA	NA	$\|0.60\|^\dagger$	NA	$\|4.06\|^\dagger$	NA	$\|5.56\|^\dagger$
$LD1$ [12]	NA	NA	NA	$\|0.91\|^\dagger$	NA	$\|0.23\|^\dagger$	NA	$\|0.14\|^\dagger$
$LD4$ [12]	NA	NA	NA	$\|0.00\|^\dagger$	NA	$\|0.00\|^\dagger$	NA	$\|0.00\|^\dagger$
EDZ_{555}	46.3445	$+1.51$	15.5229	$+0.25$	6.96904	-0.95	5.35853	-1.54
LD_{222}	45.6580	$+0.01$	15.4824	-0.01	7.03572	-0.00	5.44237	-0.00
LD_{555}	45.6531	-0.00	15.4835	$+0.00$	7.03601	$+0.00$	5.44237	-0.00
$VAPAS$	46.0669	$+0.91$	15.4066	-0.50	7.01576	-0.29	5.44215	-0.00

Table 13
Test Case 2. $\frac{E_{11\,\text{skin}}}{E_{11\,\text{core}}} \equiv FCSR = 7.3 \times 10^4$. Comparison of various theories to evaluate the transverse displacements amplitude (center plate deflection) $\widehat{u}_z = u_z \frac{100 E_{22\,\text{skin}}}{{}_zP^t h \left(\frac{a}{h}\right)^4}$ in $x = a/2$, $y = b/2$, $z = 0$.
†In Reference [12] the percentage error $Err\%$ is calculated with respect to the $LM4$ theory. In reference [12] it was not specified the formula used for the percentage error. Therefore, in this table the absolute value is used for the errors reported in reference [12]. The present error evaluations are calculated with respect to the present elasticity solution (see equation 11).

a/h	2		4		10		100	
			$\frac{E_{11\,\text{skin}}}{E_{11\,\text{core}}} \equiv FCSR = 7.3 \times 10^6$					
Elasticity	1089.86	$Err\%$	590.538	$Err\%$	149.696	$Err\%$	7.18809	$Err\%$
$LM4$ [12]	NA	NA	590.54	$+0.00$	149.70	$+0.00$	7.1881	$+0.00$
$ED4$ [12]	NA	NA	NA	$\|82.8\|^\dagger$	NA	$\|85.2\|^\dagger$	NA	$\|20.0\|^\dagger$
$EMZC3$[12]	NA	NA	NA	$\|12.5\|^\dagger$	NA	$\|3.22\|^\dagger$	NA	$\|0.03\|^\dagger$
$LD1$ [12]	NA	NA	NA	$\|14.3\|^\dagger$	NA	$\|3.93\|^\dagger$	NA	$\|0.19\|^\dagger$
$LD4$ [12]	NA	NA	NA	$\|0.00\|^\dagger$	NA	$\|0.00\|^\dagger$	NA	$\|0.00\|^\dagger$
EDZ_{555}	980.437	-10.04	581.360	-1.55	149.543	-0.10	7.19023	$+0.03$
LD_{222}	1089.20	-0.06	590.446	-0.02	149.695	-0.00	7.18809	$+0.00$
LD_{555}	1089.86	-0.00	590.538	-0.00	149.696	-0.00	7.18809	$+0.00$
$VAPAS$	4125.04	$> 100\%$	1017.25	$+72.26$	166.073	$+10.94$	7.18898	$+0.00$

Table 14
Test Case 2. $\frac{E_{11\,\text{skin}}}{E_{11\,\text{core}}} \equiv FCSR = 7.3 \times 10^6$. Comparison of various theories to evaluate the transverse displacements amplitude (center plate deflection) $\widehat{u}_z = u_z \frac{100 E_{22\,\text{skin}}}{{}_zP^t h \left(\frac{a}{h}\right)^4}$ in $x = a/2$, $y = b/2$, $z = 0$.
†In Reference [12] the percentage error $Err\%$ is calculated with respect to the $LM4$ theory. In reference [12] it was not specified the formula used for the percentage error. Therefore, in this table the absolute value is used for the errors reported in reference [12]. The present error evaluations are calculated with respect to the present elasticity solution (see equation 11).

a/h	2		4		10		100	
				$\frac{E_{11\,\text{skin}}}{E_{11\,\text{core}}} \equiv FCSR = 7.3 \times 10^8$				
Elasticity	1469.50	$Err\%$	1370.58	$Err\%$	1260.31	$Err\%$	149.506	$Err\%$
$LM4$ [12]	NA	NA	1370.6		1260.3		149.51	
$ED4$ [12]	NA	NA	NA	$\lvert 91.8\rvert^{\dagger}$	NA	$\lvert 98.1\rvert^{\dagger}$	NA	$\lvert 96.1\rvert^{\dagger}$
$EMZC3$[12]	NA	NA	NA	$\lvert 24.7\rvert^{\dagger}$	NA	$\lvert 22.5\rvert^{\dagger}$	NA	$\lvert 3.10\rvert^{\dagger}$
$LD1$ [12]	NA	NA	NA	$\lvert 27.4\rvert^{\dagger}$	NA	$\lvert 25.2\rvert^{\dagger}$	NA	$\lvert 3.82\rvert^{\dagger}$
$LD4$ [12]	NA	NA	NA	$\lvert 0.00\rvert^{\dagger}$	NA	$\lvert 0.00\rvert^{\dagger}$	NA	$\lvert 0.00\rvert^{\dagger}$
EDZ_{555}	1283.34	-12.67	1323.09	-3.47	1251.11	-0.73	149.464	-0.03
LD_{222}	1468.29	-0.08	1370.09	-0.04	1260.23	-0.01	149.507	$+0.00$
LD_{555}	1469.50	-0.00	1370.58	-0.00	1260.31	$+0.00$	149.507	$+0.00$
$VAPAS$	412009	$> 100\%$	101187	$> 100\%$	16120.2	$> 100\%$	166.591	$+11.43$

Table 15
Test Case 2. $\frac{E_{11\,\text{skin}}}{E_{11\,\text{core}}} \equiv FCSR = 7.3 \times 10^8$. Comparison of various theories to evaluate the transverse displacements amplitude (center plate deflection) $\widehat{u}_z = u_z \frac{100 E_{22\,\text{skin}}}{{}_zP^t h \left(\frac{a}{h}\right)^4}$ in $x = a/2$, $y = b/2$, $z = 0$.
†In Reference [12] the percentage error $Err\%$ is calculated with respect to the $LM4$ theory. In reference [12] it was not specified the formula used for the percentage error. Therefore, in this table the absolute value is used for the errors reported in reference [12]. The present error evaluations are calculated with respect to the present elasticity solution (see equation 11).

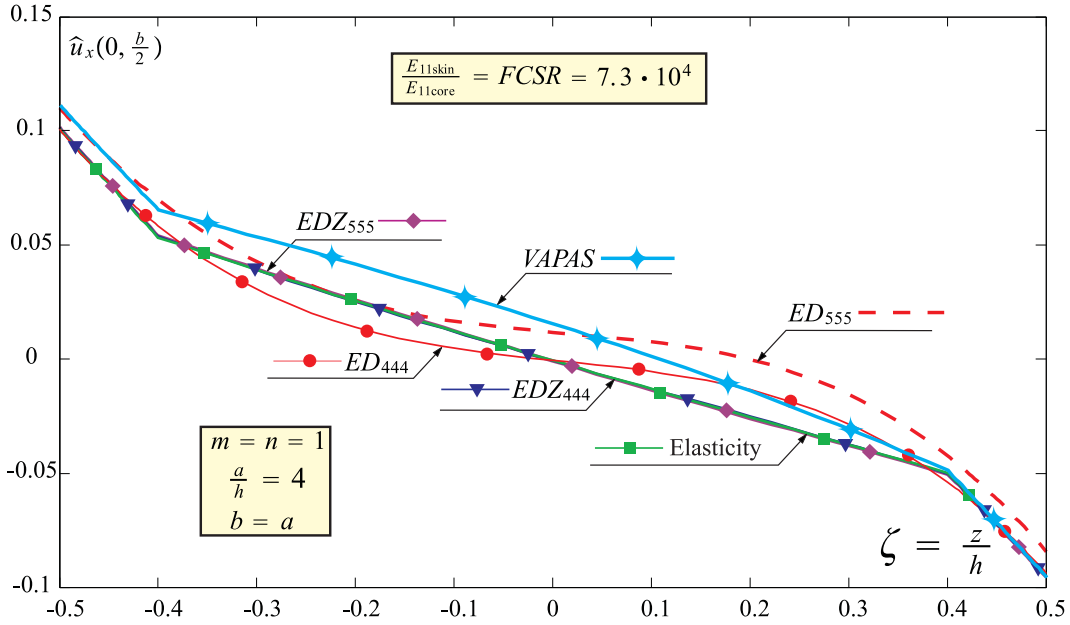

Fig. 8. Test Case 2. Dimension-less displacement $\widehat{u}_x = u_x \frac{E_{\text{skin}}}{{}_zP^t h\left(\frac{a}{h}\right)^3}$;. $\frac{E_{11\,\text{skin}}}{E_{11\,\text{core}}} \equiv FCSR = 7.3 \times 10^4$. Comparison between AHSDT, AHSDTZ, VAPAS, and the elasticity solution.

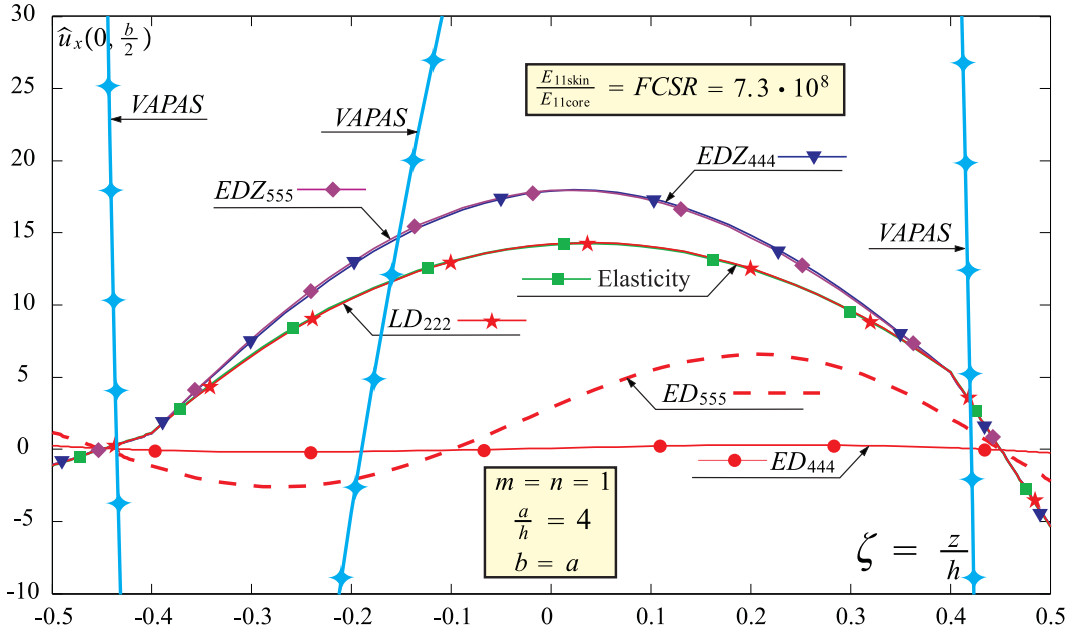

Fig. 9. Test Case 2. Dimension-less displacement $\widehat{u}_x = u_x \frac{E_{\text{skin}}}{{}_zP^t h\left(\frac{a}{h}\right)^3}$;. $\frac{E_{11\,\text{skin}}}{E_{11\,\text{core}}} \equiv FCSR = 7.3 \times 10^8$. Comparison between AHSDT, AHSDTZ, ALWT, VAPAS, and the elasticity solution.

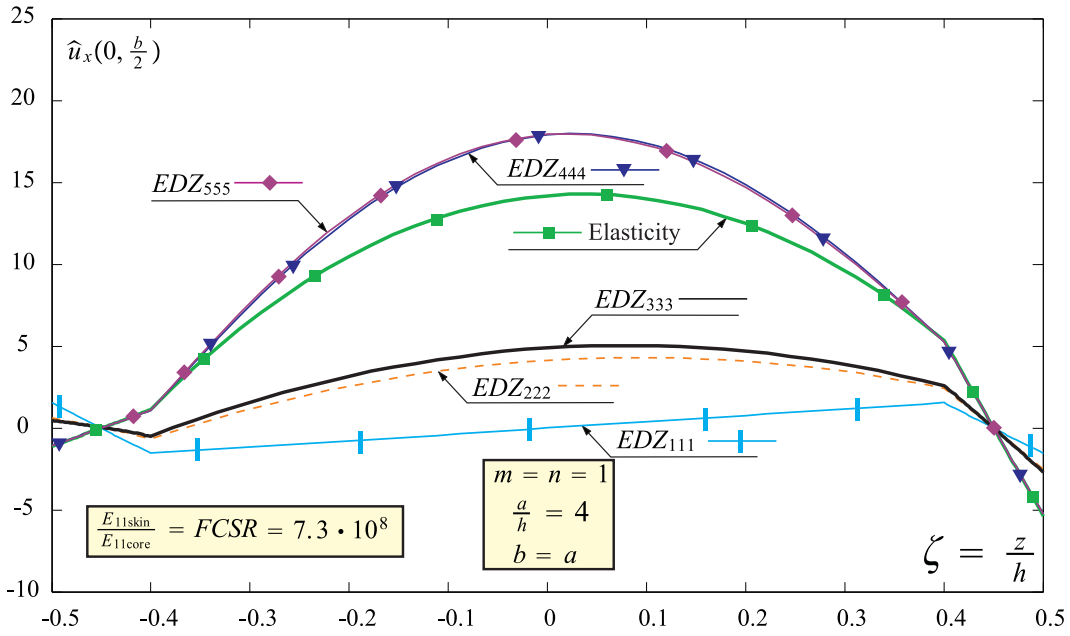

Fig. 10. Test Case 2. Dimension-less displacement $\widehat{u}_x = u_x \frac{E_{\rm skin}}{{}_zP^t h\left(\frac{a}{h}\right)^3}$;. $\frac{E_{11\,\rm skin}}{E_{11\,\rm core}} \equiv FCSR = 7.3\times 10^8$. Comparison between various zig-zag theories AHSDTZ and the elasticity solution.

5 Conclusion

The accuracy of the Variational Asymptotic Plate and Shell Analysis (VAPAS) is assessed against several higher-order, zig-zag and layerwise theories generated by using the invariant axiomatic framework denoted as Generalized Unified Formulation (GUF). Both the axiomatic models generated by GUF and VAPAS are also compared against the elasticity solution developed for the case of a sandwich structure with high Face to Core Stiffness Ratio. It has been shown that the fact that GUF allows to use an infinite number of axiomatic theories (Equivalent Single Layer theories with or without zig-zag effects and Layerwise theories as well) with any combination of orders of the displacements provides an ideal tool to precisely assess the range of applicability of the Variational Asymptotic Plate and Shell Analysis or other theories in general. It is demonstrated that VAPAS achieves accuracy comparable to a fourth (or higher) order zig-zag theory or lower-order layerwise theories, while the plate model uses the least number degrees of freedom. Hence, in comparison to the axiomatic theories, VAPAS has achieved an excellent compromise between accuracy and efficiency. Except for extreme cases of thick sandwich with huge modulus contrast, VAPAS can be used as an effective alternative to avoid expensive 3D finite element analysis for design and analysis of composite laminated plates. This assessment also points out the need that material small parameter needs to be considered to generalize the VAPAS modeling approach to deal with realistic sandwich structures.
GUF can be implemented in a single FEM code and can generate a virtually infinite number of theories with accuracy that range from the low-order equivalent single-layer to the high-order layerwise theories and is the ideal tool for comparisons and assessments of different theories or for the creation of adaptive structural codes in optimization and probabilistic studies.

Acknowledgements

The first author acknowledges the support by San Diego State University (University Grant Program).

The second author acknowledges the support by the Air Force Office of Scientific Research under Grant FA9550-08-1-0405. The program managers are Dr. Victor Giurgiutiu and Dr. David Stargel. The views and conclusions contained herein are those of the authors and should not be interpreted as necessarily representing the official policies or endorsement, either expressed or implied, of the funding agencies.

References

[1] S. A. Ambartsumian. Analysis of two-layer orthotropic shells. *nvestiia Akad Nauk SSSR, Ot Tekh Nauk*, 7, 1957.

[2] S. A. Ambartsumian. Two analysis method for two-layer orthotropic shells. *Izv An Arm SSR Seiya Fiz-Matem nauk*, X(2), 1957.

[3] S. A. Ambartsumian. On a general theory of anisotropic shells. *Prikl. Mat. Mekh.*, 22(2):226–237, 1958.

[4] S. A. Ambartsumian. On a theory of bending of anisotropic plates. *Investiia Akad Nauk SSSR, Ot Tekh Nauk*, 4, 1958.

[5] V. L. Berdichevsky. Variational-asymptotic method of constructing a theory of shells. *PMM*, 43(4):664 – 687, 1979.

[6] V. L. Berdichevsky. An asymptotic theory of sandwich plates. *International Journal of Engineering Science*, 48(3):383 – 404, 2010.

[7] E. Carrera. Evaluation of layer-wise mixed theories for laminated plates analysis. *American Institute of Aeronautics and Astronautics Journal*, 26(5):830–839, 1998.

[8] E. Carrera. Layer-wise mixed theories for accurate vibration analysis of multilayered plates. *Journal of Applied Mechanics*, 6(4):820–828, 1998.

[9] E. Carrera. Mixed layer-wise models for multilayered plates analysis. *Composite Structures*, 43(1):57–70, 1998.

[10] E. Carrera. Historical review of zig-zag theories for multilayered plates and shells. *App Mech Rev*, 56(3), 2003.

[11] E. Carrera. Theories and finite elements for multilayered plates and shells: A unified compact formulation with numerical assessment and benchmarking. *Archives of Computational Methods in Engineering*, 10(3):215–296, 2003.

[12] E. Carrera and S. Brischetto. A survey with numerical assessment of classical and refined theories for the analysis of sandwich plates. *Applied Mechanics Reviews*, 62, 2009.

[13] KN Cho, CW Bert, and AG. Striz. Free vibrations of laminated rectangular plates analyzed by higher order individual-layer theory. *Journal of Sound and Vibration*, 145:429–442, 1991.

[14] L. Demasi. Refined multilayered plate elements based on murakami zig-zag functions. *Composite Structures*, 70:308–16, 2005.

[15] L. Demasi. 2D, quasi 3D and 3D exact solutions for bending of thick and thin sandwich plates. *Journal of Sandwich Structures & MAterials*, 10(4):271–310, 2008.

[16] L. Demasi. Invariant Finite Element Model for Composite Structures: the Generalized Unified Formulation. *AIAA Journal*, 48:1602–1619, 2010.

[17] L. Demasi. Three-dimensional closed form solutions and ∞^3 theories for orthotropic plates. *Mechanics of Advanced Materials and Structures*, 17:20–39, 2010.

[18] M. E. Fares and M. Kh. Elmarghany. A refined zigzag nonlinear first-order shear deformation theory of composite laminated plates. *Composite*

Structures, 2007. doi: 10.1016/j.compstruct.2006.12.007.

[19] P. Gaudenzi, R. Barboni, and A. Mannini. A finite element evaluation of single-layer and multi-layer theories for the analysis of laminated plates. *Composite Structures*, 30:427–440, 1995.

[20] D. H. Hodges, A. R. Atılgan, and D. A. Danielson. A geometrically nonlinear theory of elastic plates. *Journal of Applied Mechanics*, 60(1):109 – 116, March 1993.

[21] T. Kant and K. Swaminathan. Free vibration of isotropic, orthotropic, and multilayer plates based on higher order refined theories. *Journal of Sound and Vibration*, 241(2):319–327, 2001.

[22] G. Kirchhoff. *Über* das gleichgewicht und die bewegung einer elastishen scheibe. *J. Angew. Math.*, 40:51 – 88, 1850.

[23] S. G. Lekhnitskii. Strength calculation of composite beams. *Vestnik inzhen i tekhnikov*, 9, 1935.

[24] L. Librescu. Improved linear theory of elastic anisotropic multilayered shells. part i. *Polymer Mechanics (translated from Russian)*, 11(6), 1975.

[25] L. Kärger, A. Wetzel, R. Rolfes, and K. Rohwer. A three-layered sandwich element with improved transverse shear stiffness and stress based on fsdt. *Computers and Structures*, 84(13-14):843 – 854, 2006.

[26] R. Mindlin. Influence of rotatory inertia and shear in flexural motion of isotropic elastic plates. *Journal of Applied Mechanics*, 18:1031 – 1036, 1951.

[27] H. Murakami. Laminated composite plate theory with improved in-plane response. *Journal of Applied Mechanics*, 53:661–666, 1986.

[28] A. Nosier, RK Kapania, and J. N. Reddy. Free vibration analysis of laminated plates using a layer-wise theory. *AIAA Journal*, pages 2335–2346, 1993.

[29] J. N. Reddy. An evaluation of equivalent single layer and layerwise theories of composite laminates. *Composite Structures*, 25:21–35, 1993.

[30] J. N. Reddy. Mechanics of laminated composite plates, theory and analysis. *(2nd edn), CRC Press.: Boca Raton, London, New York, Washington, D. C.*, 2004.

[31] E. Reissner. The effect of transverse shear deformation on the bending of elastic plates. *Journal of Applied Mechanics*, 12:69 – 76, 1945.

[32] J. G. Ren. A new theory of laminated plates. *Compos. Sci. Technol.*, 26:225–239, 1986.

[33] J.G. Ren. Bending theory of laminated plates. *Compos. Sci. Technol.*, 27:225–248, 1986.

[34] D.H. Robbins and J. N. Reddy. Modelling of thick composites using a layerwise laminate theory. *International Journal for Numerical Methods in Engineering*, 36(4):655–677, 1993.

[35] K. Swaminathan and S. S. Patil. Analytical solutions using higher order refined computational model with 12 degrees of freedom for the free vibration analysis of antisymmetric angle-ply plates. *Composite Structures*, 2007. doi: 10.1016/j.compstruct.2007.01.001.

[36] M. Tahani. Analysis of laminated composite beams using layerwise displacement theories. *Composite Structures*, 79:535–547, 2007.

[37] W. Yu. Mathematical construction of a reissner-mindlin plate theory for composite laminates. *International Journal of Solids and Structures*, 42:6680–6699, 2005.

[38] W. Yu and D. H. Hodges. An asymptotic approach for thermoelastic analysis of laminated composite plates. *Journal of Engineering Mechanics*, 130(5):531 – 540, 2004.

[39] W. Yu, D. H. Hodges, and V. V. Volovoi. Asymptotic construction of Reissner-like models for composite plates with accurate strain recovery. *International Journal of Solids and Structures*, 39(20):5185 – 5203, 2002.

[40] W. Yu, D. H. Hodges, and V. V. Volovoi. Asymptotically accurate 3-D recovery from Reissner-like composite plate finite elements. *Computers and Structures*, 81(7):439 – 454, 2003.

[41] Wu Zhen, Y. K. Cheung, S. H. Lo, and Chen Wanji. Effects of higher-order global-local shear deformations on bending, vibration and buckling of multilayered plates. *Composite Strutures*, 2007. DOI: 10.1016/j.compstruct.2007.01.017.